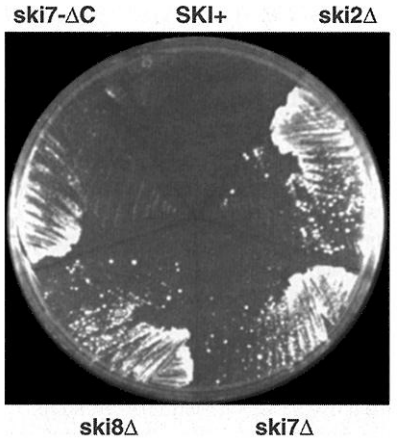

Fig. 4. Nonstop mRNA degradation is effective in limiting the translation of aberrant mRNAs. The *HIS3* gene was amplified by polymerase chain reaction using oRP1075 (CGAGAGCTCAACACAGTCCTTTCCCGCAA) and oRP1077 (CGAGGATCCACTTGCCACCTATCACC) and was cloned as a Sac I–Bam HI fragment into the CEN URA3 plasmid pRS416 (*30*). The nonstop *his3* allele was created by deleting the first nucleotide of the termination codon (Quick-change kit, Stratagene). This creates an open reading frame that extends past the previously mapped polyadenylation sites (*31*). The nonstop his3 plasmid was transformed into strains that were ura3Δ and his3Δ and were either SKI+, ski2Δ, ski7Δ. ski8Δ, or ski7-ΔC. URA+ transformants were selected and streaked onto a plate lacking histidine. This plate is shown after a 2-day incubation at 30°C.

mRNA degradation pathway, protein products of nonstop mRNAs accumulate to functional levels.

In combination, these results define a mechanism of mRNA quality control that recognizes and degrades yeast mRNAs lacking translation codons, thereby preventing the production of truncated proteins. Because Ski protein homologs are present in the human genome (*19*, *26*), we expect that the mechanism of nonstop decay is conserved. Transcripts that lack a termination codon are also recognized in prokaryotes (*15*, *16*). It will be interesting to determine to what extent the prokaryotic and eukaryotic systems are similar and whether they are evolutionarily related.

References and Notes

1. P. Hilleren, R. Parker, *RNA* **5**, 711 (1999).
2. P. A. Frischmeyer *et al.*, *Science* **295**, 2258 (2002).
3. D. Muhlrad, C. J. Decker, R. Parker, *Genes Dev.* **8**, 855 (1994).
4. C. Beelman *et al.*, *Nature* **382**, 577 (1996).
5. M. Tucker *et al.*, *Cell* **104**, 377 (2001).
6. J. S. Jacobs Anderson, R. Parker, *EMBO J.* **17**, 1497 (1998).
7. A. van Hoof, R. Parker, *Cell* **99**, 347 (1999).
8. P. Mitchell, D. Tollervey, *Nature Struct. Biol.* **7**, 843 (2000).
9. A. van Hoof, R. R. Staples, R. E. Baker, R. Parker, *Mol. Cell. Biol.* **20**, 8230 (2000).
10. J. Brown, X. Bai, A. W. Johnson, *RNA* **6**, 449 (2000).
11. Y. Araki *et al.*, *EMBO J.* **20**, 4684 (2001).
12. D. Muhlrad, C. J. Decker, R. Parker, *Mol. Cell. Biol.* **15**, 2145 (1995).
13. Nonstop mRNAs are not detectably deadenylated, even when they are stabilized by deletion of SKI7 or several other exosome mutations. One possible explanation is that a stalled ribosome occupies the extreme 3′ end of this mRNA and prevents exonucleases from digesting it. A corollary of this explanation is that in a wild-type strain, the exosome or associated proteins can dislodge a stalled ribosome at the 3′ end of the mRNA or initiate 3′-to-5′ decay of the mRNA in the presence of such a ribosome.
14. To test whether translation of nonstop PGK1 mRNA was required in cis, we introduced G_{18} in its 5′ UTR. This sequence forms a stable secondary structure and reduces translation by 4 orders of magnitude (*27*). This reduction in translation severely reduced exosome-mediated decay of the nonstop PGK1 mRNA (half-life = 14 min).
15. A. W. Karzai, E. D. Roche, R. T. Sauer, *Nature Struct. Biol.* **7**, 449 (2000).
16. A. Muto, C. Ushida, H. Himeno, *Trends Biochem. Sci.* **23**, 25 (1998).
17. L. Benard, K. Carroll, R. C. Valle, D. C. Masison, R. B. Wickner, *J. Virol.* **73**, 2893 (1999).
18. The SKI7 homology with translation factors is most evident in the GTPase domain, but multiple sequence alignment shows that the homology extends to the COOH-terminus of Ski7p, EF1A, and eRF3 (*19*).
19. Supplemental data can be found on *Science* Online at www.sciencemag.org/cgi/content/full/295/5563/2262/DC1.
20. Alleles encoding either a COOH-terminal truncation or an NH_2-terminal deletion of Ski7p were integrated into the genome at the SKI7 locus and were expressed from the SKI7 promoter. The NH_2-terminal deletion removed amino acids 18 through 239, whereas the COOH-terminal truncation removed all amino acids from 265 to the COOH-terminal. The COOH-terminal truncation removes all of the translation factor homology.
21. Hemagglutinin (HA)–tagged Ski7p was generated as described (*28*) and introduced into strains that carried a protein A–tagged version of Rrp4p (*29*), Ski4p, or Rrp6p, which are subunits of the exosome. As a control, we used a similarly HA-tagged version of Ski3p, which is known not to copurify with the exosome (*10*). All five tagged proteins are expressed from their normal genomic locus and are functional (*22*). Ski3p, Ski4p, Ski7p, and Rrp6 are also expressed from their own promoters, whereas Rrp4p is expressed from the GAL10 promoter (*29*). Protein extracts were prepared by vortexing in the presence of glass beads and 50 mM Tris-HCl (pH 7.5), 50 mM NaCl, 2 mM $MgCl_2$, 1 mM β-mercaptoethanol, 0.1% NP40, and complete protease inhibitors EDTA free (Roche) and were incubated at 4°C for 1 hour with immunoglobulin G (IgG)–Sepharose beads. The beads were then washed twice with 40 volumes of the extraction buffer and twice with 40 volumes of the extraction buffer containing 1 M NaCl. The proteins bound to the IgG-Sepharose were recovered by boiling in sample buffer.
22. A. van Hoof, P. A. Frischmeyer, H. C. Dietz, R. Parker, data not shown.
23. C. Allmang *et al.*, *Genes Dev.* **13**, 2148 (1999).
24. K. T. Burkard, J. S. Butler, *Mol. Cell. Biol.* **20**, 604 (2000).
25. R. Pulak, P. Anderson, *Genes Dev.* **7**, 1885 (1993).
26. C.-Y. Chen *et al.*, *Cell* **107**, 455 (2001).
27. D. Muhlrad, C. J. Decker, R. Parker, *Mol. Cell. Biol.* **15**, 2145 (1995).
28. M. S. Longtine *et al.*, *Yeast* **14**, 953 (1998).
29. P. Mitchell, E. Petfalski, D. Tollervey, *Genes Dev.* **10**, 502 (1996).
30. R. S. Sikorski, P. Hieter, *Genetics* **122**, 19 (1989).
31. S. Mahadevan, T. R. Raghunand, S. Panicker, K. Struhl, *Gene* **190**, 69 (1997).
32. We thank the members of the Parker laboratory for insightful comments and A. Sachs for antibodies to Lsm1p. Funded by the Howard Hughes Medical Institute.

19 October 2001; accepted 31 January 2002

Brain to Plasma Amyloid-β Efflux: a Measure of Brain Amyloid Burden in a Mouse Model of Alzheimer's Disease

Ronald B. DeMattos,[1,2,3]* Kelly R. Bales,[5]* David J. Cummins,[5] Steven M. Paul,[5,6]† David M. Holtzman[1,2,3,4]†

The deposition of amyloid-β (Aβ) peptides into amyloid plaques precedes the cognitive dysfunction of Alzheimer's disease (AD) by years. Biomarkers indicative of brain amyloid burden could be useful for identifying individuals at high risk for developing AD. As in AD in humans, baseline plasma Aβ levels in a transgenic mouse model of AD did not correlate with brain amyloid burden. However, after peripheral administration of a monoclonal antibody to Aβ (m266), we observed a rapid increase in plasma Aβ and the magnitude of this increase was highly correlated with amyloid burden in the hippocampus and cortex. This method may be useful for quantifying brain amyloid burden in patients at risk for or those who have been diagnosed with AD.

Abundant evidence suggests that a key event in the pathogenesis of AD is the conversion of Aβ peptides from soluble to insoluble forms in the brain (*1*). This process is among the earliest pathological changes that characterizes AD, and is estimated to occur ~10 to 20 years before the appearance of the earliest cognitive changes of the disease (*2*, *3*). Whereas individuals with pre-clinical AD (i.e., cognitively normal individuals with plaque and tangle densities similar to those with AD) have no measurable neuronal loss in affected brain regions, individuals with even very mild cognitive impairment indica-

tive of clinical AD have plaques and tangles and also have already lost a significant number of neurons (*4*, *5*). Identification of biomarkers predictive of the presence and magnitude of amyloid plaque burden may be useful in the diagnosis of both pre-clinical and clinical AD. In the case of pre-clinical AD, these biomarkers might allow for detection of individuals who may benefit from preventative therapies even before the development of neuronal loss and cognitive impairment. Further, such biomarkers may be of help in distinguishing patients with mild cognitive impairment (MCI) due to AD and those with other underlying disease processes.

The Aβ peptides are predominantly 40 to 42 amino acids in length and are synthesized as soluble proteolytic products of the amyloid precursor protein (APP), a large integral membrane protein expressed at high levels in the brain (*1*). Recent data suggest that after Aβ synthesis in the central nervous system (CNS), the peptide(s) can be locally metabolized or cleared into the plasma (*6*–*9*). With the use of a tg mouse model of AD amyloidosis, PDAPP (APP^{V717F}) mice, in which a human *APP* transgene with a familial AD mutation is expressed (*10*), we have recently demonstrated that peripheral administration of a monoclonal antibody to Aβ (m266) results in a rapid and massive increase of CNS-derived Aβ in the plasma (*9*). Our data suggested that m266 was both decreasing plasma Aβ degradation as well as facilitating Aβ efflux from CNS to plasma. The presence and amount of insoluble Aβ deposited in plaques in the brain appears to influence the metabolism and clearance of soluble Aβ. For example, as plaque deposition progresses, the amount of insoluble Aβ in brain lysates increases markedly (*11*). Though the amount of soluble Aβ in brain lysates does not increase to the same extent, it does increase (*12*). Thus, we reasoned that the accumulation of Aβ in plasma after the administration of m266 might be a measure of (or in some way reflect the amount of) Aβ burden in the brain.

We assessed a large cohort (n = 49) of PDAPP mice homozygous (+/+) for the APP^{V717F} transgene, all of which were 12 to 13 months of age. These mice begin to exhibit Aβ and amyloid deposition in the brain at ~3 to 6 months of age. Though all $PDAPP^{+/+}$ mice ultimately develop deposits of Aβ in the form of diffuse and neuritic (thioflavine-S-positive, amyloid) plaques after 6 months, there is a rather large variability in the degree of amyloid pathology in individual animals of the same age (*9*, *13*, *14*). This inherent variability in amyloid burden in our age-matched cohort allowed us to compare plasma Aβ levels with brain Aβ burden. Five minutes before administering m266 to the mice, we obtained a baseline plasma sample from each animal. Each mouse then received an intravenous (i.v.) injection of m266 (500 μg). Plasma samples from each animal were then obtained 5 min and 1, 3, 6, and 24 hours later. In each plasma sample, levels of $Aβ_{40}$ and $Aβ_{42}$ were assessed by enzyme-linked immunosorbent assay (ELISA) as previously described (*9*). Mice were killed after 24 hours. One hemisphere was assessed with the use of quantitative Aβ-immunofluorescent and thioflavine-S (amyloid) staining to determine the area of the hippocampus or cingulate cortex occupied by Aβ and amyloid, respectively (% Aβ or amyloid load), and regions from the other hemisphere were assessed for Aβ by ELISA as described (*9*, *14*, *15*). Neuropathological assessment of Aβ and amyloid load was carried out by investigators blind to the plasma Aβ levels.

Baseline levels of plasma $Aβ_{40}$, $Aβ_{42}$, and the calculated $Aβ_{40/42}$ ratio before the administration of m266 did not correlate with the amount of Aβ or amyloid deposition present in the brain (Table 1, Fig. 1). This finding is similar to that previously reported in humans where plasma Aβ has been shown not to be a useful biomarker in distinguishing AD patients from age-matched controls (*16*). As we have previously reported, after parenteral (i.v.) administration of m266, there was a rapid and marked increase in plasma $Aβ_{40}$ and $Aβ_{42}$. We also observed highly significant correlations between levels of plasma Aβ ($Aβ_{40}$, $Aβ_{42}$, $Aβ_{40/42}$ ratio) and both Aβ and amyloid burden in the hippocampus (Fig. 1, Table 1) and in the cingulate cortex. In addition, highly significant correlations were observed when comparing the total amount of plasma $Aβ_{40}$ and $Aβ_{42}$ accumulated over 24 hours (area under the curve, AUC) and both Aβ and amyloid burden (Table 1). Highly significant correlations were obtained when comparing plasma Aβ levels after m266 ad-

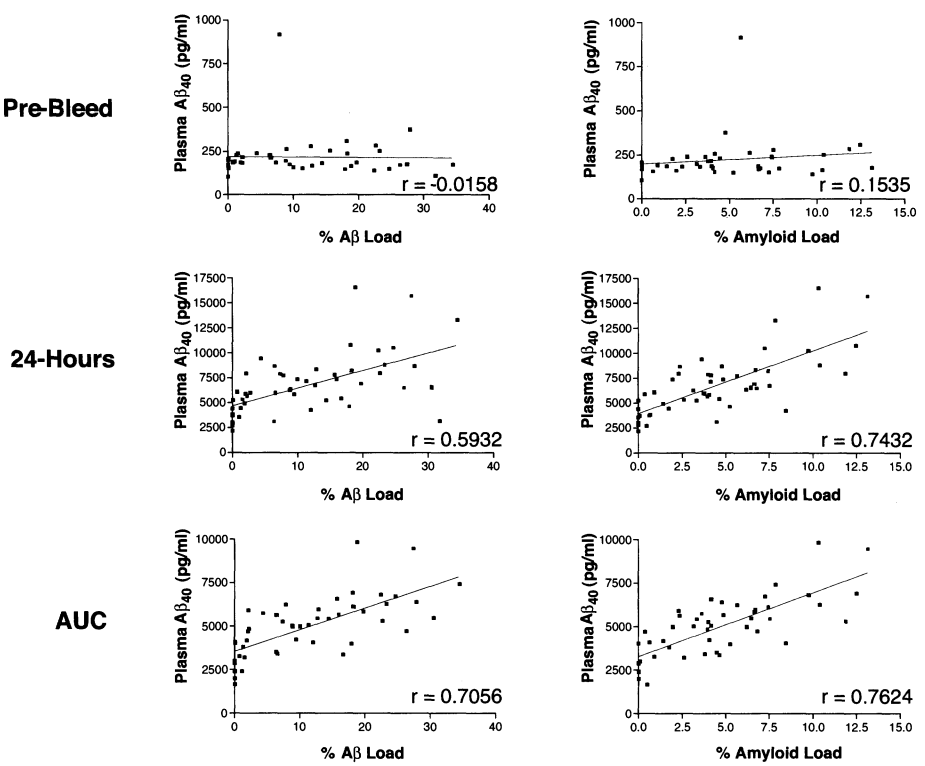

Fig. 1. Plasma levels of $Aβ_{40}$ following m266 administration are highly correlated with Aβ and amyloid burden in hippocampus. Just before (pre-bleed) and after the i.v. administration of m266 (500 μg), plasma samples were collected at various times (1, 3, 6, and 24 hours). Plasma $Aβ_{40}$ and $Aβ_{42}$ were measured by ELISA as previously described (9). Aβ and amyloid load were quantitated as described (*14*). Before m266 administration, there was no correlation between the plasma levels of $Aβ_{40}$ (or $Aβ_{42}$) (Table 1) and % Aβ or amyloid load in the hippocampus. In contrast, 24 hours after i.v. administration of m266, there were highly significant correlations (see Table 1) when comparing the plasma levels of $Aβ_{40}$ and the $Aβ_{40}$ accumulation over 24 hours (AUC) to Aβ and amyloid load in the hippocampus.

[1]Center for the Study of Nervous System Injury, [2]Alzheimer's Disease Research Center, [3]Department of Neurology, [4]Molecular Biology and Pharmacology, Washington University School of Medicine, 660 South Euclid Avenue, Box 8111, St. Louis, MO 63110, USA. [5]Neuroscience Discovery Research, Eli Lilly and Co., Lilly Research Laboratories, Indianapolis, IN 46285, USA. [6]Departments of Pharmacology, Toxicology, and Psychiatry, Indiana University School of Medicine, Indianapolis, IN 46285, USA.

*These authors contributed equally to this work.
†To whom correspondence should be addressed. E-mail: holtzman@neuro.wustl.edu (D.M.H.) or Paul_Steven_M@Lilly.com (S.M.P.)

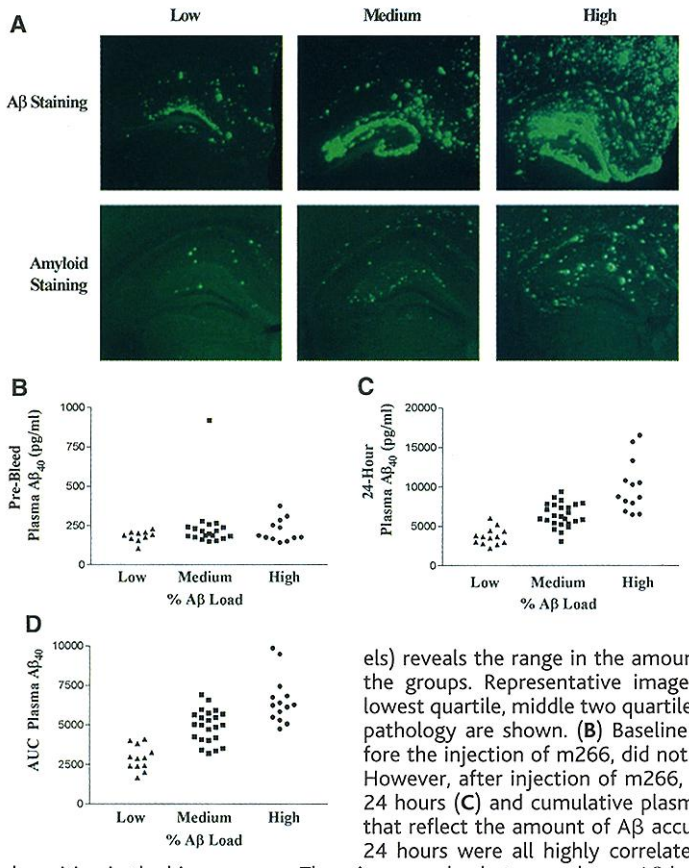

Fig. 2. PDAPP +/+ mice (12 to 13 months of age) with varying amounts of Aβ deposition can be differentiated by plasma Aβ measurements after the parenteral (i.v.) administration of m266. (**A**) Mice were divided into quartiles based on Aβ load in the hippocampus: the lowest quartile of hippocampal Aβ load (low, 0 to 1.4% Aβ load), the middle two quartiles of Aβ load (medium, 1.4 to 18.2% Aβ load), and the highest quartile of Aβ load (high, 18.2 to 34.5%). Aβ-immunofluorescent staining (top panels) and thioflavine-S (amyloid) staining (bottom panels) reveals the range in the amount of deposition between the groups. Representative images from a mouse in the lowest quartile, middle two quartiles, and highest quartile of pathology are shown. (**B**) Baseline plasma $A\beta_{40}$ levels, before the injection of m266, did not differentiate the groups. However, after injection of m266, plasma $A\beta_{40}$ levels after 24 hours (**C**) and cumulative plasma $A\beta_{40}$ levels (AUC) (**D**) that reflect the amount of Aβ accumulating in plasma over 24 hours were all highly correlated to the amount of Aβ deposition in the hippocampus. There is no overlap between plasma Aβ levels in the low versus the high Aβ load groups after m266 administration (C) and (D).

Table 1. Plasma Aβ correlations with Aβ load and fibrillar amyloid in hippocampus with AD-like pathology. The Pearson correlation coefficient (Pearson r) and significance (*P* value) were determined between plasma Aβ values (before and after injection of m266) and hippocampal Aβ or amyloid load with the use of GraphPad Prism software (v. 3.00 for Windows, San Diego, CA). Aβ load was defined as the % area of the hippocampus covered by Aβ-immunoreactive deposits. Amyloid load was defined as the % area of the hippocampus covered by thioflavine-S positive deposits. Correlations were also determined between the plasma Aβ accumulation over 24 hours (AUC) and hippocampal Aβ load or amyloid load.

	Pre-bleed	5 min	1 hour	3 hours	6 hours	24 hours	AUC
				Plasma $A\beta_{40}$			
Aβ load							
Pearson r	−0.0158	0.5527	0.5904	0.4310	0.5533	0.5932	0.7056
P value	0.9209	<0.0001	<0.0001	<0.0014	<0.0001	<0.0001	<0.0001
Amyloid load							
Pearson r	0.1535	0.7420	0.6257	0.7053	0.6684	0.7432	0.7624
P value	0.3378	<0.0001	<0.0001	<0.0001	<0.0001	<0.0001	<0.0001
				Plasma $A\beta_{42}$			
Aβ Load							
Pearson r	−0.0614	0.2223	−0.0036	0.1309	0.4551	0.3391	0.5322
P value	0.6817	0.1207	0.9798	0.3549	0.0008	0.0139	<0.0001
Amyloid load							
Pearson r	0.0443	0.4790	0.2321	0.3996	0.4476	0.6062	0.6214
P value	0.7698	0.0005	0.1013	0.0037	0.0011	<0.0001	<0.0001
				$A\beta_{40/42}$ *ratio*			
Aβ Load							
Pearson r	0.0369	0.5223	0.6888	0.4215	0.1754	0.7190	0.6138
P value	0.8236	<0.0001	<0.0001	0.0019	0.2183	<0.0001	<0.0001
Amyloid load							
Pearson r	0.1293	0.4825	0.5047	0.4364	0.2843	0.6029	0.5510
P value	0.4393	0.0004	0.0002	0.0014	0.0454	<0.0001	<0.0001

ministration to brain Aβ levels measured by ELISA. We next grouped mice according to their Aβ burden and compared plasma Aβ levels among those with the lowest, middle two, and highest quartiles of Aβ burden (Fig. 2A). There was no overlap in plasma $A\beta_{40}$ levels assessed at 24 hours (or in AUC for plasma $A\beta_{40}$) after m266 administration between mice in the lowest quartile (0 to 1.4%) versus those in the highest quartile (18.2 to 34.5%) of brain Aβ load (Fig. 2, A, C, and D). By contrast, plasma Aβ levels measured just before m266 administration failed to differentiate these two groups of mice (Fig. 2B).

To further explore whether measuring plasma Aβ levels after m266 administration could potentially be used to develop a diagnostic test to estimate brain Aβ or amyloid burden, we used recursive-partitioning, an exploratory statistical technique for revealing rule-based relations in data (*17*, *18*). This technique generates a set of hierarchical "rules" which can be graphically displayed as a tree dendogram (decision tree). To develop predictive models, we examined all plasma Aβ values after m266 administration in relation to Aβ burden in the hippocampus. Using diagnostic rules based on only one plasma Aβ measurement [$A\beta_{40}$ at 24 hours (*19*)] or on multiple measurements (*19*), several models were generated that accurately predicted the levels of hippocampal Aβ burden (*19*). We next developed a rule-based "diagnostic" procedure whereby, after the administration of an antibody to Aβ, the presence of "high" or "low" plaque burden could be predicted with acceptable false-negative and false-positive rates for such a test. Using a decision tree, one model allowed us to discriminate between animals with greater than the 50% percentile of Aβ burden in the cohort (n = 49) from those with less than that percentile, with a sensitivity of 96% and a specificity of 84%. The recursive-partitioning models discussed were intentionally forced to be very conservative, which suggests that more complex models with even higher predictive power can be developed for eventual use in humans.

Here, we found no correlation between baseline levels of plasma Aβ and brain Aβ burden in a large cohort of 12-to 13-month-old PDAPP mice. In contrast, after parenteral administration of m266, we observed rapid and large increases in plasma $A\beta_{40}$, $A\beta_{42}$, and the $A\beta_{40/42}$ ratio that were highly correlated with the amount of Aβ deposition and amyloid burden in brain. There was no overlap between plasma $A\beta_{40}$ levels at 24 hours after m266 administration in mice from the lowest and highest quartiles of Aβ burden quantitated in the hippocampus. Our findings have obvious implications for quantifying Aβ and/or amyloid burden in humans. However, whether such a "diagnostic" test in humans would yield similar results is unclear. Though there is a

wide range of Aβ and amyloid deposition that occurs with age in both humans and PDAPP mice, all PDAPP mice overproduce human Aβ and, unlike humans, all mice will eventually develop Aβ and amyloid deposition in the brain. In quantitative terms, this contrasts with what is observed in the aging human brain. Whereas cortical amyloid plaque burden in humans with pre-clinical and clinical AD are similar to each other and to that observed in the PDAPP mice we studied with high Aβ burden, studies have shown that most cognitively normal elderly humans (~70% by age 75) have either no or only very small amounts of cortical Aβ deposition (*3*, *20*). The latter human group would be analogous to the mice in our study with little to no Aβ deposition (lowest quartile). This dichotomy in amyloid plaque burden observed in the aging human brain suggests, therefore, that measuring plasma Aβ after administration of antibody to Aβ may be able to clearly distinguish such individuals. Thus, the use of a monoclonal antibody with characteristics similar to m266 but developed for humans may provide a means to develop a facile diagnostic test to quantify amyloid burden in persons with pre-clinical AD, as well as to assist in the differential diagnosis of clinical AD. Such a test may also have utility for monitoring the response to anti-amyloid therapy.

The highly significant correlations between plasma Aβ and both brain Aβ and amyloid burden strongly suggest that the presence of m266 in the peripheral circulation directly facilitated net Aβ efflux from the brain, acting as a "peripheral sink." Further supporting this model is that significant correlations were observed within 5 min after peripheral injection of m266. By increasing Aβ efflux from brain, it appears that the presence of m266 in plasma can also reveal quantitative differences in brain Aβ deposition, presumably by facilitating efflux of soluble Aβ from brain. Taken together, our data suggest that brain Aβ clearance is a dynamic process and that modifying this process may be useful in both diagnosing and treating AD.

References and Notes

1. D. J. Selkoe, *Physiol. Rev.* **81**, 741 (2001).
2. H. Yamaguchi, S. Sugihara, A. Ogawa, N. Oshima, Y. Ihara, *J. Neuropathol. Exp. Neurol.* **60**, 731 (2001).
3. J. L. Price, J. C. Morris, *Ann. Neurol.* **45**, 358 (1999).
4. T. Gomez-Isla *et al.*, *J. Neurosci.* **16**, 4491 (1996).
5. J. L. Price *et al.*, *Arch. Neurol.* **58**, 1395 (2001).
6. J.-F. Ghersi-Egea *et al.*, *J. Neurochem.* **67**, 880 (1996).
7. M. Shibata *et al.*, *J. Clin. Invest.* **106**, 1489 (2000).
8. Y. Ji, B. Permanne, E. M. Sigurdsson, D. M. Holtzman, T. Wisniewski, *J. Alzheimer's Dis.* **3**, 23 (2001).
9. R. B. DeMattos *et al.*, *Proc. Natl. Acad. Sci. U.S.A.* **98**, 8850 (2001).
10. D. Games *et al.*, *Nature* **373**, 523 (1995).
11. J. Wang, D. W. Dickson, J. Q. Trojanowski, V. M. Y. Lee, *Exp. Neurol.* **158**, 328 (1999).
12. J. Naslund *et al.*, *JAMA* **283**, 1571 (2000).
13. Supplemental data are available on *Science* Online at www.sciencemag.org/cgi/content/full/295/5563/2264/DC1.
14. C. E. Fishman *et al.*, *J. Neurosci. Methods* **108**, 145 (2001).
15. D. M. Holtzman *et al.*, *Proc. Natl. Acad. Sci. U.S.A.* **97**, 2892 (2000).
16. P. D. Mehta *et al.*, *Arch. Neurol.* **57**, 100 (2000).
17. L. Breiman, J. Friedman, R. Olshen, X. Stone, *Classification and Regression Trees* (CRC Press, Boca Raton, FL, 1984).
18. For more information see: www.recursive-partitioning.com/Bibliography/.
19. See Web fig. 2 (*13*).
20. J. C. Morris *et al.*, *Neurology* **46**, 707 (1996).

21. The authors wish to acknowledge the technical assistance of X. Wu, C. DeLong, M. Parsadanian, and M. O'Dell and the helpful comments of J. Morris, E. Johnson, R. Dean, P. May, T. Augsberger-Brown, and D. Choi. Supported by Eli Lilly and Co. D.M.H. is also supported by National Institute on Aging (grant AG20222).

30 October 2001; accepted 13 February 2002

Dynamics of Pleistocene Population Extinctions in Beringian Brown Bears

I. Barnes,[1,2] P. Matheus,[3] B. Shapiro,[2] D. Jensen,[2*] A. Cooper[2†]

The climatic and environmental changes associated with the last glaciation (90,000 to 10,000 years before the present; 90 to 10 ka B.P.) are an important example of the effects of global climate change on biological diversity. These effects were particularly marked in Beringia (northeastern Siberia, northwestern North America, and the exposed Bering Strait) during the late Pleistocene. To investigate the evolutionary impact of these events, we studied genetic change in the brown bear, *Ursus arctos*, in eastern Beringia over the past 60,000 years using DNA preserved in permafrost remains. A marked degree of genetic structure is observed in populations throughout this period despite local extinctions, reinvasions, and potential interspecies competition with the short-faced bear, *Arctodus simus*. The major phylogeographic changes occurred 35 to 21 ka B.P., before the glacial maximum, and little change is observed after this time. Late Pleistocene histories of mammalian taxa may be more complex than those that might be inferred from the fossil record or contemporary DNA sequences alone.

Throughout the late Pleistocene Beringia formed a largely ice-free subcontinent connecting the Old and New Worlds. This period saw a number of major events including global climatic change, the movement of humans into the New World (~13 ka B.P.), and a large-scale extinction of megafauna (~12 to 10 ka B.P.). Preliminary studies of mammal bones preserved in permafrost deposits have shown that genetic information can be retrieved from material aged more than 60 ka B.P., beyond the limit of radiocarbon dating (*1–4*). To study genetic change in large-mammal populations throughout this period, we examined 71 brown bears preserved in east Beringian permafrost and cave deposits, comprising all suitable specimens available in museums. Brown bears were chosen because their extensive modern distribution in Europe, Asia, and North America shows strong phylogeographic structuring (*5–7*), and they are thought to have entered Eastern Beringia early in the last (Wisconsinan) glaciation (*8*). In North America, three genetically and geographically distinct clades of brown bears (2, 3, and 4) are currently recognized (Figs. 1 and 2D) as well as several subclades (3a, 3b, 2a), one of which consists of the polar bear [*U. maritimus*, 2b (*7*)]. Studies suggest that much of this structure may have resulted from expansions following glacial population bottlenecks, and that late Pleistocene populations were considerably more diverse genetically (*2*).

DNA was obtained from cortical bone samples (~0.5 g) of 36 specimens by established ancient-DNA techniques (*9*). Two sections of the mitochondrial (mt) control region, 135 and 60 base pairs (bp), respectively, were amplified by polymerase chain reaction (PCR). Primer pairs were chosen to amplify short yet highly variable regions of mtDNA, to maximize ancient-DNA recovery while allowing the detection of population turnover through time. The phylogenetic relationships of brown bear clades have been previously established with the use of longer sequences (*7*). Stratigraphic control is often lacking for permafrost bones, so radiocar-

[1]Institute of Biological Anthropology, University of Oxford, Oxford OX2 6QS, UK. [2]Henry Wellcome Ancient Biomolecules Centre, Department of Zoology, University of Oxford, Oxford OX1 3PS, UK. [3]Alaska Quaternary Center, University of Alaska, Fairbanks, AK 99775, USA.

*Present address: United Nations Environment Program–Balkans, International Environment House, Chemin des Anémones 15, 1219 Châtelaine, Geneva, Switzerland.

†To whom correspondence should be addressed. E-mail: alan.cooper@zoo.ox.ac.uk